两个二亚胺–铜(I)-膦配合物的合成、结构和太赫兹时域光谱

朱 宁[1,2] 潘 迅[1] 林 森[1] 杨玉平[3] 辛秀兰[4] 李中峰[1] 张 帆*,[1] 金琼花*,[1,2]
([1] 首都师范大学化学系,北京 100048)
([2] 中国科学院福建物质结构研究所,结构化学国家重点实验室,福州 350002)
([3] 中央民族大学理学院,北京 100081)
([4] 北京工商大学食品学院,北京 100048)

摘要：本文报道了 2 个新的 Cu(I)配合物：[Cu(PPh₃)₂(dppz)]I (**1**)(PPh₃=三苯基膦,dppz=二吡啶并[3,2-a:2′,3′-c]吩嗪)和[Cu₂(dppm)₂(dppz)₂]Cl₂ (**2**)(dppm=双(二苯基膦)甲烷)的合成,并通过 X 射线单晶衍射、元素分析、核磁共振氢(膦)谱、荧光光谱和太赫兹时域光谱对其进行了分析和表征。分析结果显示配合物 **1** 是一个单核配合物,中心 Cu(I)离子与 2 个含膦配体(PPh₃)和 1 个含氮配体(dppz)进行配位,形成了一个扭曲的四面体结构。与 **1** 不同的是,配合物 **2** 是由 CuCl,dppm 和 dppz 以 1:1:1 的比例混配得到的双核配合物。其中,双膦配体 dppm 作为桥联配体,连接了 2 个 Cu(I)离子。荧光光谱表明所有的发射峰均源于金属到配体的电荷转移跃迁(MLCT)。同时,使用太赫兹时域光谱技术表征了 2 种配合物以及相应的配体。

关键词：铜(I)配合物；结构；荧光；太赫兹时域光谱；二吡啶并[3,2-a:2′,3′-c]吩嗪

Syntheses, Structures and Terahertz Time-Domain Spectroscopy of Two Diimine-Copper(I)-Phosphine Complexes

ZHU Ning[1,2] PAN Xun[1] LIN Sen[1] YANG Yu-Ping[3] XIN Xiu-Lan[4]
LI Zhong-Feng[1] ZHANG Fan*,[1] JIN Qiong-Hua*,[1,2]
([1]*Department of Chemistry, Capital Normal University, Beijing 100048, China*)
([2]*State Key Laboratory of Structural Chemistry, Fujian Institute of Research on the Structure of Matter, Chinese Academy of Sciences, Fuzhou 350002, China*)
([3]*School of Science, Minzu University of China, Beijing 100081, China*)
([4]*School of Food and Chemical Engineering, Beijing Technology and Business University, Beijing 100048, China*)

Abstract: Herein, two novel copper(I) complexes, [Cu(PPh₃)₂(dppz)]I (**1**) and [Cu₂(dppm)₂(dppz)₂]Cl₂ (**2**) (PPh₃=triphenylphosphine, dppz=dipyrido [3,2-a:2′,3′-c]phenazine, dppm=bis (diphenylphosphino)methane) have been synthesized, and the characterization of the complexes was carried out through single-crystal X-ray diffraction, elemental analysis, IR, ¹H/³¹P NMR spectroscopy, fluorescence spectra and THz time domain spectroscopy (THz-TDS). The results show that **1** is a mononuclear complex. The central Cu(I) builds a distorted tetrahedral geometry by coordinating with two phosphine ligands (PPh₃) and one chelating N-donor ligand (dppz). Different from **1**, **2** exhibits a dinuclear structure which was obtained by the reaction of CuCl and dppm with dppz in 1:1:1 molar ratio, where the diphosphine ligand (dppm) was utilized as a bridging ligand coordinating to two copper(I) atoms. The luminescent spectra show that the emission mechanism belongs to metal-to-ligand charge transfer

(MLCT). At the same time, the terahertz (THz) time-domain spectroscopy was used to represent these two complexes as well as the corresponding ligands. CCDC: 1558489, **1**; 1915009, **2**.

0   Introduction

The photoluminescence of metal complexes has been widely studied in recent years for their promising potential in optical sensor[1-3], solar energy conversion[4-6], biological systems[7-9] and organic light-emitting diodes (OLEDs)[10-15]. Through systematic study on the variation of ligands, structural and bonding modes of different metal centres, the structure-property relationships of various classes of luminescent transitional metal complexes can be obtained. In this respect, Cu(I) complexes play an important role in devices that require high quantum efficiency[16-18]. Compared with traditional precious metals like iridium, ruthenium, and so on [19-20], copper is abundant in nature and low in cost. At the same time, different Cu(I) salts and special ligands can be adopted around the central copper to control the structure of Cu(I) complexes as well as improve their luminous performances[21].

Heteroleptic Cu(I) complexes of the [Cu(N^N)(P^P)]⁺ type system have been developed, which can exhibit impressive performance, e.g., long-lived excited-state, high emission quantum yield with tunable emission spectra[22-25]. According to previous literatures, it is obvious to find that steric effects have the strongest impact on luminescent properties, because large and rigid ligands can suppress the flattening distortion for complexes in emissive state[26-29]. Based on this point, dipyrido [3,2-*a*:2′,3′-*c*]phenazine (dppz) was found as a noticeable bidentate N-donor ligand. The bulky aromatic ring can furnish large steric hindrance and sequentially keep the complex in its original tetrahedral geometry. In accordance with the hard and soft acid-base (HSAB) theory, dipyrido[3,2-*a*:2′,3′-*c*]phenazine (dppz) can easily coordinate with Cu(I) centre, which proves theoretically that dppz can serve as a resultful ligand to synthesize Cu(I) complexes.

In this paper, two novel Cu(I) complexes with dppz ligands have been reported. According to pre-existing literatures and former researches in our group[30-32], the introducion of phosphine ligands can improve the luminescent property and enhance the stability of Cu(I) complexes. On the basis of these results, we added triphenylphosphine (PPh₃) and bis(diphenylphosphino)methane (dppm) as phosphine ligands to the system and synthesized two heteroleptic Cu(I) complexes, $[Cu(PPh_3)_2(dppz)]I$ (**1**) and $[Cu_2(dppm)_2(dppz)_2]Cl_2$ (**2**). We also used X-ray diffraction, elemental analysis, ¹H/³¹P NMR spectroscopy, fluorescence spectra and THz time-domain spectroscopy (THz-TDS)[30,33] to characterize their structures and investigated the emission and fluorescence properties.

1   Experimental

1.1   Materials and measurements

All commercially available starting reagents were used without any purification. FT-IR spectra (KBr pellets) were measured on a Perkin-Elmer Infrared spectrometer. C, H and N elemental analysis were carried out on an Elementar Vario MICRO CUBE (Germany) elemental analyzer. Room-temperature fluorescence spectra were measured on F-4500 FL Spectrophotometer. ¹H NMR was recorded at room temperature with a Bruker DPX 600 spectrometer. The THz absorption spectra were recorded on a THz time domain device of Minzu University of China, carried out in a N_2 atmosphere to avoid the influence of water vapor, based on photoconductive switches for the generation and electro-optical crystal detection of the far-infrared light, effective frequency in the range 0.2~2.8 THz.

1.2   Synthesis of [Cu(PPh₃)₂(dppz)]I (1)

A mixture of CuI (0.038 1 g, 0.2 mmol), dppz (0.056 4 g, 0.2 mmol) and PPh₃ (0.104 9 g, 0.4 mmol) were dissolved in the mixed solvents of 5 mL CH_2Cl_2

and 5 mL CH_3OH. The mixture was stirred for 6 hours and filtered. Yellow crystal **1** was obtained from the filtrate after standing at room temperature for several days. Yield: 75%. Element analysis Calcd. for $C_{54}H_{40}CuIN_4P_2$(%): C, 65.03; H, 4.03; N, 5.62. Found(%): C, 64.98; H, 3.98; N, 5.77. IR data (cm^{-1}, KBr pellets): 3 434w, 3 053w, 1 630w, 1 572s, 1 488s, 1 435s, 1 414 m, 1 357m, 1 337s, 1 071m, 819s, 736m, 695w, 523w. ^1H NMR (600 MHz, DMSO-d_6, 298 K): δ 9.65 (m, CH from dppz), 9.02 (dd, CH from dppz), 8.47 (dd, CH from dppz), 8.15 (dd, CH from dppz), 8.05 (dd, CH from dppz), 7.38 (m, $CH_{benzene}$ from PPh$_3$), 7.31 (d, $CH_{benzene}$ from PPh$_3$), 7.21 (d, $CH_{benzene}$ from PPh$_3$); ^{31}P NMR (243 MHz, DMSO-d_6, 298K): δ −1.31 (s, phosphorus from PPh$_3$).

1.3　Synthesis of $[Cu_2(dppm)_2(dppz)_2]Cl_2$ (2)

Complex **2** was prepared in a manner similar to the described for **1**, using CuCl (0.019 8 g, 0.2 mmol), dppz (0.056 4 g, 0.2 mmol) and dppm (0.076 9 g, 0.2 mmol) as starting materials in a mixture of CH_2Cl_2 (5 mL) and CH_3OH (5 mL). Yield: 55%. Element analysis Calcd. for $C_{68}H_{64}Cu_2Cl_2N_8P_4$(%): C, 62.01; H, 4.85; N, 8.53. Found(%): C, 62.05; H, 4.87; N, 8.52. IR data (cm^{-1}, KBr pellets): 3 426w, 3 049w, 1 630w, 1 573w, 1 488s, 1 434m, 1 416s, 1 432s, 1 358m, 1 338m, 1 074 m, 824m, 738m, 694m, 515s, 480s. ^1H NMR (600 MHz, DMSO-d_6, 298K): δ 9.55 (d, CH from dppz), 9.17 (s, CH from dppz), 8.40 (s, CH from dppz), 8.08 (s, CH from dppz), 7.98 (s, CH from dppz), 7.43 (m, $CH_{benzene}$ from PPh$_3$), 7.16 (m, $CH_{benzene}$ from PPh$_3$), 7.04 (s, $CH_{benzene}$ from PPh$_3$); ^{31}P NMR (243 MHz, DMSO-d_6, 298K): δ −1.18 (s, phosphorus from dppm).

1.4　Structure determination

Single crystals of the title complexes were mounted on a Bruker Smart 1000 CCD diffractometer equipped with a graphite-monochromated Mo $K\alpha$ (λ = 0.071 073 nm) radiation at 298 K. Semi-empirical absorption corrections were applied using SADABS programs[34]. All the structures were solved by direct methods using SHELXS program of the SHELXTL-97 package and refined with SHELXL-97[35]. Metal atom centers were located from the E-maps and other non-hydrogen atoms were located in successive difference Fourier syntheses. The final refinements were performed by full matrix least-squares methods with anisotropic thermal parameters for non-hydrogen atoms on F^2. The hydrogen atoms were generated geometrically and refined with displacement parameters riding on the concerned atoms.

Crystallographic data and experimental details for structural analysis are summarized in Table 1, and selected bond lengths and angles of complexes **1**~**2** are summarized in Table 2.

CCDC: 1558489, **1**; 1915009, **2**.

Table 1　Crystallographic data for complexes 1~2

		Complex **1**	Complex **2**
	Formula	$C_{54}H_{40}CuIN_4P_2$	$C_{68}H_{64}Cu_2Cl_2N_8P_4$
	Formula weight	997.28	1 531.31
	Crystal system	Triclinic	Monoclinic
	Space group	$P\bar{1}$	$C2/c$
	Crystal size / mm	0.31×0.20×0.14	0.40×0.37×0.30
	a / nm	1.086 29(2)	3.942 2(3)
	b / nm	1.476 87(1)	1.306 3(1)
	c / nm	1.683 23(1)	2.019 9(1)
	α / (°)	95.391(1)	
	β / (°)	102.695(2)	118.233(3)
	γ / (°)	110.791(3)	
	V / nm^3	2.418 7(3)	9.164 3(1)
	Z	2	4
	D_c / (g·cm^{-3})	1.369	1.110
	$F(000)$	1 008	3 152

Continued Table 1

Goodness-of-fit on F^2	1.072	1.078
R_{int}	0.024 8	0.096 6
R_1 [$I>2\sigma(I)$][a]	0.065 0	0.080 8
wR_2 [$I>2\sigma(I)$][b]	0.204 1	0.180 3
R_1 (all data)[a]	0.099 2	0.161 1
wR_2 (all data)[b]	0.222 1	0.196 0

[a] $R=\sum ||F_o|-|F_c||/ \sum |F_o|$; [b] $wR=[\sum w(|F_o|^2-|F_c|^2)^2/ \sum w(F_o^2)]^{1/2}$.

**Table 2   Selected bond distances (nm) and bond angles (°) for complexes 1~2**

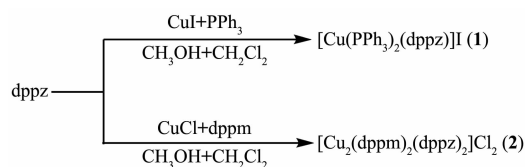| Complex **1**					
Cu(1)-P(1)	0.230(1)	Cu(1)-N(1)	0.214(4)		
Cu(1)-P(2)	0.230(1)	Cu(1)-N(2)	0.211(5)		
P(1)-Cu(1)-P(2)	125.52(6)	N(2)-Cu(1)-P(1)	109.88(4)	N(1)-Cu(1)-P(1)	109.65(3)
N(2)-Cu(1)-P(2)	109.20(4)	N(1)-Cu(1)-P(2)	113.29(3)	N(2)-Cu(1)-N(1)	79.97(7)
Complex **2**					
Cu(1)-P(1)	0.226(1)	Cu(1)-N(1)	0.211(5)		
Cu(1)-P(2)	0.223(1)	Cu(1)-N(2)	0.210(5)		
P(1)-Cu(1)-P(2)	135.63(6)	N(2)-Cu(1)-P(1)	98.02(4)	N(1)-Cu(1)-P(1)	101.09(3)
N(2)-Cu(1)-P(2)	121.15(4)	N(1)-Cu(1)-P(2)	105.64(4)	N(2)-Cu(1)-N(1)	79.3(2)

2   Results and discussion

2.1   Synthesis of the complexes

Both complexes were synthesized using the same N-heteroaromatic ligands dipyrido [3,2-a:2′,3′-c]phenazine (dppz) and different phosphine ligands by one-pot reaction. The previous literatures[28] show that solvents have non-negligible impact on the terminal structure of complexes. Thus, we chose mixed solvent of CH_3OH and CH_2Cl_2 (1:1, V/V) and added triphenylphosphine in the synthesis of complex **1** (Scheme 2). Complex **2** was prepared in a similar manner as described for **1**, except that bis (diphenylphosphino)methane was used in place of triphenylphosphine. Complexes **1** and **2**

triphenylphosphine (PPh$_3$)   1,1-bis(diphenylphosphino)methane (dppm)   dipyrido[3,2-a:2′,3′-c]phenazine (dppz)
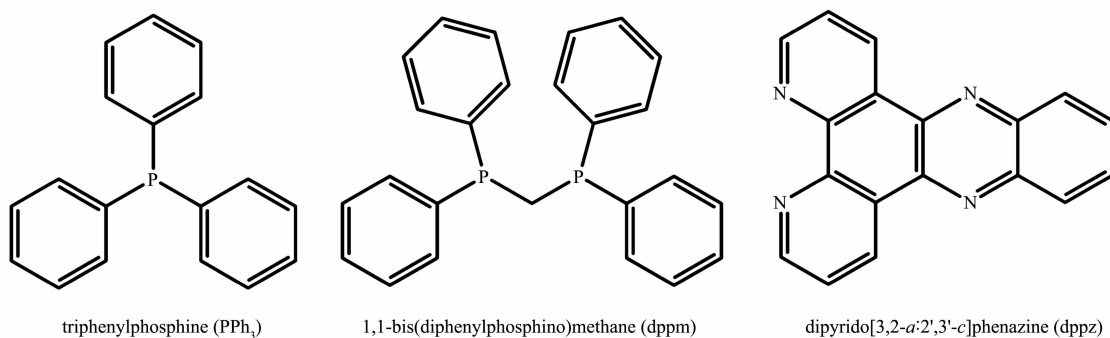
Scheme 1   Structures of the ligands used in the present work

Scheme 2   Routes of syntheses for complexes **1** and **2**

are mononuclear and dinuclear structures, respectively. Both of them are stable in air and can be stored for a long term.

2.2 Description of crystal structures

Fig.1 shows the molecular structure of complex **1**. X-ray analysis clearly reveals that **1** crystallizes in the triclinic crystal system with space group $P\bar{1}$ and adopts a typical mononuclear tetrahedral coordination geometry for Cu(Ⅰ) ion, where Cu(Ⅰ) is surrounded by two P atoms from triphenylphosphine (PPh$_3$) ligands and two N atoms from dipyrido[3,2-a:2′,3′-c]phenazine (dppz) ligand. The Cu-N bond lengths range from 0.211 3(5) to 0.214 0(4) nm and Cu-P from 0.229 83(17) to 0.230 09(17) nm, which are slightly different from those of [Cu(PPh$_3$)$_2$(DPPZ)]BF$_4$[36] (Cu-N bond lengths range from 0.206 9 to 0.210 5 nm and Cu-P from 0.227 2 to 0.227 5 nm) and [Cu(PPh$_3$)$_2$(dppz)]NO$_3$[37] (The average bond lengths of Cu-N and Cu-P are 0.209 6 and 0.227 2 nm, respectively). This difference may be due to the replacement between CuBF$_4$/CuNO$_3$ and CuI. The bond angles were listed in Table 2, which means that Cu(Ⅰ) ion occupies a distorted tetrahedral coordination center.

According to previous literatures[36-37], Cu(Ⅰ) complexes with large coplanar conjugation planes, such as the inter- or intra-molecular π-π stacking, can contribute to a formation of complex molecules in solid state, showing a head-to-head dual-molecule structure. Besides, π-π stacking possibly stabilizes and protects the excited state of Cu(Ⅰ) complexes from being attacked by external molecule and suppresses the probability of quenching[38]. However, similar to the complex [Cu(PPh$_3$)$_2$(dppz)]BF$_4$, no such π-π stacking or head-to-head dual-molecule structure was found in solid state [Cu(PPh$_3$)$_2$(dppz)]I. This left the copper exposed and vulnerable to attack by peripheral molecules, increasing the possibility of quenching.

The crystal packing of complex **1** reveals that unit cell forms two-dimensional supramolecular networks as depicted in Fig.2. The above 2D structure is supported by C−H⋯π interactions (C16⋯Cg(1) 0.270 nm; C29⋯Cg(2) 0.291 nm; C39⋯Cg(3) 0.259 nm) between neighboring molecules, which play a critical role in structure orientation.

Complex **2** crystallizes in the monoclinic crystal system with space group $C2/c$ and its molecular structure is depicted in Fig.3. It consists of a neutral dimeric molecular unit with two copper atoms bridged by a pair of dppm ligands and forms an eight-membered Cu$_2$P$_4$C$_2$ ring. Besides, each Cu(Ⅰ) centre terminally
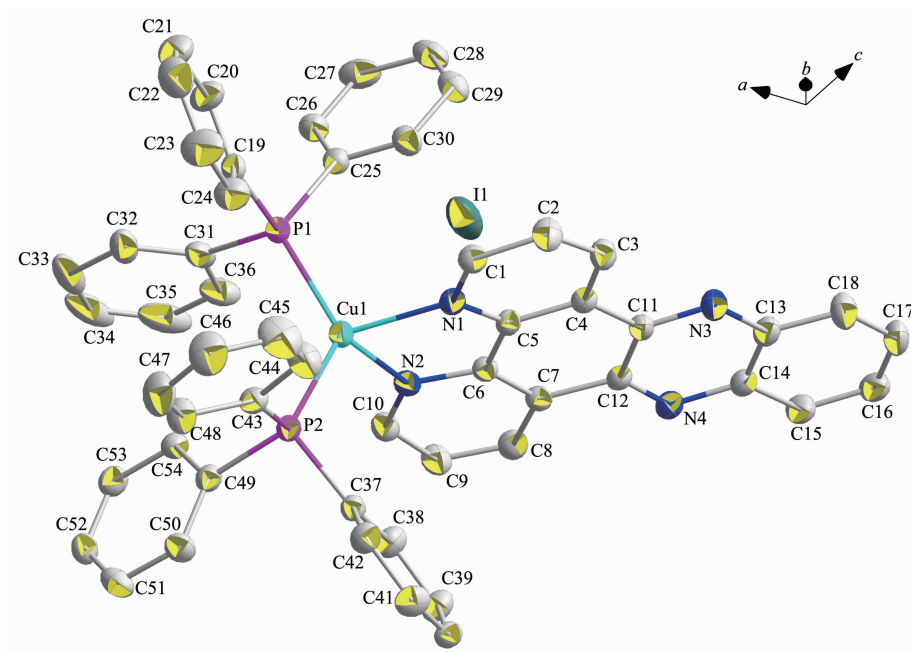
All hydrogen atoms are omitted for clarity; Thermal ellipsoids are drawn at 30% probability level

Fig.1 Molecular structure of complex **1**

chelates with two nitrogen atoms of dppz. The Cu-P bond lengths ranging from 0.222 9 to 0.226 23 nm are similar to those of normal [Cu(dppm)(P^P)]⁺ complexes[39]. The Cu···Cu separation of 0.365 2 nm is significantly longer than the range of copper-copper bond length, suggesting that copper atoms in complex **2** are not involved in metal-metal bonding interactions. The P(1)-Cu(1)-P(2) angle (104.95(4)°) is similar to the

Most hydrogen atoms, all anions and a part of phenyl rings are omitted for clarity; Symmetry codes: i −x, −y, 1−z; ii 1−x, 1−y, 1−z; iii −x, −y, −z

Fig.2　Two-dimensional networks of complex **1**

All hydrogen atoms are omitted for clarity; Thermal ellipsoids drawn at 30% probability level; Symmetry code: iv 0.5−x, 0.5−y, 1−z

Fig.3　Molecular structure of complex **2**

corresponding complex $[Cu(dppm)(MeCN)_2]_2(ClO_4)_2$ [40]. In summary, Cu(I) in complex **2** is a similar distorted tetrahedral coordination centre as **1**, and only the presence of bridging ligand (dppm) results in the formation of a binuclear complex.

2.3　^1H NMR and ^{31}P NMR spectroscopy

　　The ^1H NMR spectra of complexes **1** and **2** were measured at room temperature in DMSO-d_6. The ^1H NMR spectrum of complex **1** exhibited signals (multiple peaks) between 9.65 and 8.05 (δ), which can be assigned to protons from the aromatic rings of dppz ligand ((δ: 9.65, 2H, dd, J=8.1Hz), (δ: 9.02, 2H, dd, J_1=8.1 Hz, J_2=1.5 Hz), (δ: 8.47, 2H, dd, J_1=6.5 Hz, J_2=3.4 Hz), (δ: 8.15, 2H, dd, J_1=6.6 Hz, J_2=3.3 Hz), (δ: 8.05, 2H, dd, J_1=8.1 Hz, J_2=4.8 Hz)). In complex **1**, the signals at a δ range of 7.38~7.21 are attributed to protons from PPh_3 ((δ: 7.38, 6H, m), (δ: 7.31, 12H, d), (δ: 7.21, 12H, d)), respectively. As for complex **2**, the signals at a δ range of 9.65~7.98 belong to heterocyclic hydrogen from dppz ((δ: 9.55, 4H, d, J=7.8 Hz), (δ: 9.17, 4H, s), (δ: 8.40, 4H, s), (δ: 8.08, 4H, s), (δ: 7.98, 4H, s)) and dppm ((δ: 7.43, 8H, m), (δ: 7.16, 16H, m), (δ: 7.04~6.99, 16H, t)), respectively. While the ^{31}P NMR spectra of complexes **1** and **2** exhibit single signals at −1.31 and −1.18 (δ) can be ascribed to phosphorus of the diphosphine ligands, respectively.

2.4　Fluorescence spectra

　　Fig.4 presents the solid-state emission spectra of complexes **1** and **2** which were measured at room temperature. Upon excitation at 408 nm, complex **1** displayed emission at 612 nm with a broad band peak. Compared with $[Cu(PPh_3)_2(dppz)]BF_4$ [37], it stays slightly blue-shifted about 17 nm in the short wave direction, which may result from the I^- replacing BF_4^-. In comparison with **1**, complex **2** exhibited weak solid-state emission centered at 604 nm under excitation at 402 nm, which red-shifts 8 nm compared to **1**. For the same ligands in complexes **1** and **2**, it is observed that the enlarged conjugation plane in dppz has an important influence on Cu(I) complexes. On the one hand, the large steric hindrance can suppress the flattening in tetrahedral structure; on the other hand, the enlarged conjugation increases the delocalization

of electrons on the ligand, which will decrease the quantum yields and destroy the luminescent performance. Compared with the corresponding ligands, all of complexes show strong red-shifted of emission maximum, which may be attributed to metal-to-ligand charge transfer luminescent emission between the central Cu(I) and ligands.
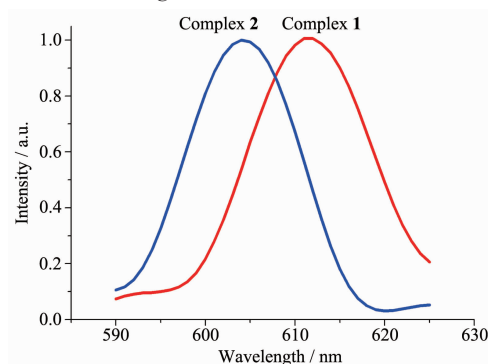

Fig.4　Luminescent spectra of complexes **1** and **2** in the solid state at 298 K

2.5　Terahertz time domain spectroscopy (THz-TDS)

　　The terahertz time-domain spectroscopy (THz-TDS) of PPh_3, dppm, dppz and complexes **1**~**2** were measured in a range of 0.2~2.8 THz at room temperature. All the above compounds had characteristic resonance peaks, which may be explained by the fact that in polar molecules the dipoles rotate and vibrate, resulting in strong absorption and chromatic dispersion. The peaks found for them were as follows: PPh_3: 0.26, 1.00, 1.25, 1.32, 1.70, 1.90, 2.02, 2.29, 2.49, 2.64 THz (Fig.5); dppm: 0.47, 0.73, 0.88, 1.00, 1.14, 1.26, 1.52, 1.64, 2.16, 2.28, 2.55, 2.61 THz (Fig.6); dppz: 0.26, 0.88, 1.00, 1.26, 1.38, 1.43, 1.52, 1.64, 1.78, 1.90, 1.95, 2.02, 2.16, 2.23, 2.28, 2.34, 2.46, 2.55, 2.66 THz (Fig.7); complex **1**: 0.26, 0.74, 0.86, 1.02, 1.43, 1.58, 1.74, 1.87, 1.93, 2.08, 2.20, 2.28, 2.52, 2.63, 2.69, 2.78 THz (Fig.8); complex **2**: 0.23, 0.34, 0.42, 1.45, 1.75, 1.93, 2.03, 2.17, 2.29, 2.36, 2.48, 2.69 THz (Fig.9). The phosphine ligands PPh_3 and dppm are non-polar molecules, and the weak peaks appearing in the terahertz time-domain spectra are attributed to the tiny skeleton vibration of the unit cell as a whole. The absorption peaks present in dppz are attributed to $\pi \cdots \pi$ stacking existing between

conjugate planes. By comparing the THz absorption spectra of the products with those of the reactants, some phenomena can be found that most peaks of the ligands disappeared or moved in the complexes. New peaks appearing in the complexes indicate that the

THz absorption spectra are associated with the coordination of copper ions and the ligands. According to the previous study of our group, the absorption peaks of complex **1** at 1.43~2.52 THz are related to the C−H···π intermolecular weak force. There are big differences in THz absorption spectra of complexes **1** and **2** because of the effect of different coordinating phosphine ligands and terminal geometry structures. Although the correspondence between the crystal structures and observed spectra does not allow a definitive characterization, it is possible to make tentative assignments of many of the observed features in the terahertz region for the samples. The results in this work are a supplement to the THz spectroscopic properties of Cu(I) complexes containing nitrogen and phosphorous ligand.
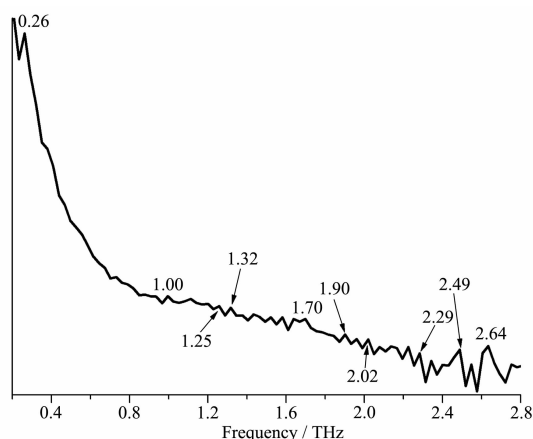

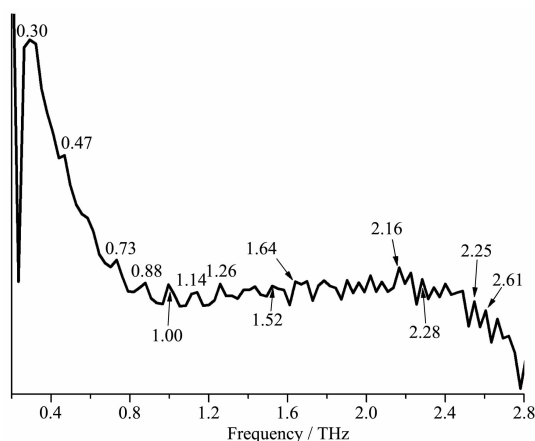Fig.5　Terahertz spectrum of PPh$_3$ in a range of 0.2~2.8 THz

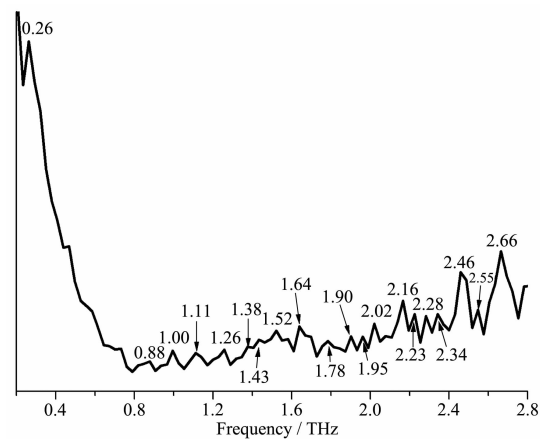Fig.6　Terahertz spectrum of dppm in a range of 0.2~2.8 THz

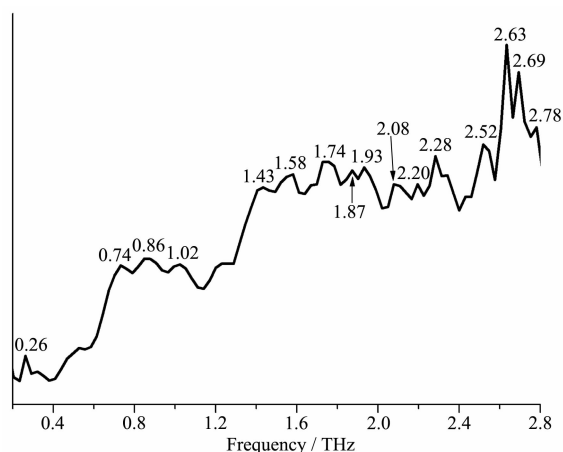Fig.7　Terahertz spectrum of dppz in a range of 0.2~2.8 THz

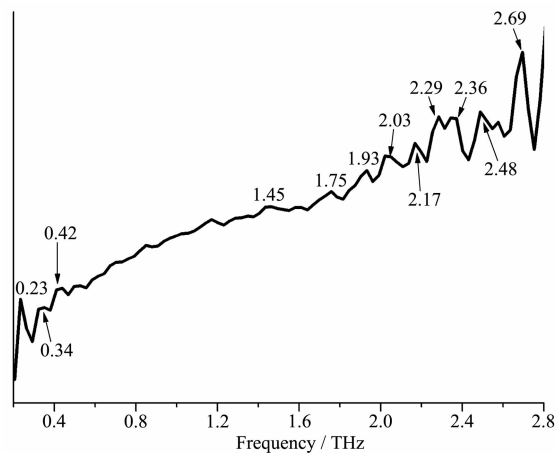Fig.8　Terahertz spectrum of complex **1** in a range of 0.2~2.8 THz

Fig.9　Terahertz spectrum of complex **2** in a range of 0.2~2.8 THz

3　Conclusions

Two novel Cu(I) complexes, namely [Cu(PPh$_3$)$_2$(dppz)]I (**1**) and [Cu$_2$(dppm)$_2$(dppz)$_2$]Cl$_2$ (**2**), have been synthesized and characterized by single-crystal X-ray diffraction, elemental analysis, ^{1}H/^{31}P NMR spectroscopy, fluorescence spectra and THz time-domain spectroscopy (THz-TDS). **1** is a mononuclear complex and **2** is a dinuclear complex because of its bridging phosphine ligands. Both of their emission peaks are derived from metal-to-ligand charge transfer (MLCT). All the complexes show great stability, which can be used in optical materials and luminescence research. The application of THz time domain spectroscopy (THz-TDS) provides useful information for researching the structure and luminescence of compounds.

References:

[1] dos Santos C M G, Harte A J, Quinn S J, et al. *Coord. Chem. Rev.*, **2008**,**252**:2512-2527

[2] Hu X, Wang F Y, Peng Q Q, et al. *RSC Adv.*, **2019**,**9**:13048-13053

[3] Farahani Y D, Safarifard V. *J. Solid State Chem.*, **2019**,**275**:131-140

[4] Jana M K, Janke S M, Dirkes D J, et al. *J. Am. Chem. Soc.*, **2019**,**141**:7955-7964

[5] Hayashi T, Kobayashi A, Ohara H, et al. *Inorg. Chem.*, **2019**,**54**:8905-8913

[6] Huang X S, Hu M, Zhao X H, et al. *Org. Lett.*, **2019**,**21**:3382-3386

[7] Cao L D, Zhang H R, Zhou Z L, et al. *Nanoscale*, **2018**,**10**:20354-20365

[8] Taha Z A, Ajlouni A M, Al Momani W. *J. Lumin.*, **2012**,**132**:2832-2841

[9] Gao H, Zhao X, Chen S J. *Molecules*, **2018**,**23**:419/1-419/20

[10]Zhang D D, Duan L. *J. Phys. Chem. Lett.*, **2019**,**10**:2528-2537

[11]Tsuboyama A, Kuge K, Furugori M, et al. *Inorg. Chem.*, **2007**,**46**:1992-2001

[12]Xiao L, Chen Z, Qu B, et al. *Adv. Mater.*, **2011**,**23**:926-952

[13]Hashimoto M, Igawa S, Yashima M, et al. *J. Am. Chem. Soc.*, **2011**,**133**:10348-10351

[14]Minaev B, Jansson E, Agren H, et al. *J. Chem. Phys.*, **2006**,**125**:234704

[15]Helander M G, Wang Z B, Qiu J, et al. *Science*, **2011**,**332**:944-947

[16]Hamze R, Peltier J L, Sylvinson D, et al. *Science*, **2019**,**363**:601-606

[17]Brunner F, Martinez-Sarti L, Keller S, et al. *Dalton Trans.*, **2016**,**45**:15180-15192

[18]Linfoot C L, Leitl M J, Richardson P, et al. *Inorg. Chem.*, **2014**,**53**:10854-10861

[19]Adachi C, Baldo M A, Thompson M E, et al. *J. Appl. Phys.*, **2001**,**90**:5048-5051

[20]Tanaka D, Agata Y, Takeda T, et al. *Jpn. J. Appl. Phys.*, **2007**,**46**:L117-L119

[21]Zhang Y, Schulz M, Waechtler M, et al. *Coord. Chem. Rev.*, **2018**,**356**:127-146

[22]Kuang S M, Cuttell D G, McMillin D R. *Inorg. Chem.*, **2002**,**41**:3313-3322

[23]Zhang Q S, Zhou Q G, Cheng Y X, et al. *Adv. Mater.*, **2004**,**16**:432-436

[24]Bergmann L, Friedrichs J, Mydlak M, et al. *Chem. Commun.*, **2013**,**49**:6501-6503

[25]Chen X L, Yu R M, Zhang Q K, et al. *Chem. Mater.*, **2013**,**25**:3910-3920

[26]Mara M W, Jackson N E, Huang J, et al. *J. Phys. Chem. B*, **2013**,**117**:1921-1931

[27]Garakyaraghi S, Danilov E O, McCusker C E, et al. *J. Phys. Chem. A*, **2015**,**119**:3181-3193

[28]McCusker C E, Castellano F N. *Inorg. Chem.*, **2013**,**52**:8114-8120

[29]Green O, Gandhi B A, Burstyn J N. *Inorg. Chem.*, **2009**,**48**:5704-5714

[30]Kuang X N, Lin S, Liu J M, et al. *Polyhedron*, **2019**,**165**:51-62

[31]PAN Xun(潘迅), KUANG Xiao-Nan(匡晓楠), ZHU Ning(朱宁), et al. *Chinese J. Inorg. Chem.*(无机化学学报), **2019**,**35**:361-368

[32]Zhang Y R, Yu X, Lin S, et al. *Polyhedron*, **2017**,**138**:46-56

[33]Wang Y, Kuang X N, Cui Y Z. *Polyhedron*, **2018**,**155**:135-143

[34]Sheldrick G M. *SHELXTL NT Ver.*5.1, University of Göttingen, Germany, **1997**.

[35]Sheldrick G M. *SHELXS*-97 and *SHELXL*-97, Madison, WI, USA, **1997**.

[36]Zhang L M, Yue S M, Li B, et al. *Inorg. Chim. Acta*, **2012**,**384**:225-232

[37]Villarreal W, Colina-Vegas L, Visbal G, et al. *Inorg. Chem.*, **2017**,**56**:3781-3793

[38]Chen H F, Hung W Y, Chen S W, et al. *Inorg. Chem.*, **2012**,**51**:12114-12121

[39]Tsukuda T, Nakamura A, Arai T, et al. *Bull. Chem. Soc. Jpn.*, **2006**,**79**:288-290

[40]Ruina Y, Kunhua L, Yimin H, et al. *Polyhedron*, **1997**,**16**:4033-4038